Evidence for a highly deformed band in $^{12}C+^{16}O$ breakup of ^{28}Si

N. I. Ashwood, J. T. Murgatroyd, N. M. Clarke, M. Freer, B. R. Fulton, and A. St. J. Murphy
School of Physics and Astronomy, University of Birmingham, Edgbaston, Birmingham B15 2TT, United Kingdom

S. P. G. Chappell, R. L. Cowin, G. K. Dillon, and D. L. Watson
Department of Physics, University of York, York YO1 5DD, United Kingdom

W. N. Catford, N. Curtis, and M. Shawcross
School of Physics and Chemistry, University of Surrey, Guildford, Surrey GU2 5XH, United Kingdom

V. Pucknell
CLRC Daresbury Laboratory, Daresbury, Warrington, Cheshire WA4 4AD, United Kingdom
(Received 14 August 2000; published 20 February 2001)

The $^{16}O(^{16}O,^{12}C^{16}O)\alpha$ reaction has been studied at incident energies of 90 and 97 MeV. States in ^{28}Si are reconstructed over the excitation energy range 22–45 MeV, and the spins of six states, ranging from 9^- to 17^-, were obtained from angular correlation measurements. A comparison of these breakup states with scattering resonances indicates that some of the breakup states lie below the locus of the $^{12}C+^{16}O$ scattering resonances, and may belong to a highly deformed band with a rotational parameter of (42 ± 5) keV and a bandhead energy of $E_x=(26.3\pm0.9)$ MeV.

DOI: 10.1103/PhysRevC.63.034315 PACS number(s): 21.10.Hw, 25.70.Ef, 27.30.+t

I. INTRODUCTION

In the last decade much evidence has emerged for a link between the resonances observed in the elastic scattering of alpha-conjugate light heavy ions such as $^{12}C+^{12}C$ and $^{16}O+^{16}O$ [1–3] and the excited states of the respective compound nuclei seen in symmetric cluster breakup initiated via various reactions [4–9]. Early breakup studies used inelastic scattering to excite the incident heavy ions and invariant mass or resonant particle spectroscopy [10] to obtain the excitation energy of the states in the compound nucleus; the spins of the states can also be determined using angular correlation techniques [11–14]. A high resolution study of the $^{12}C+^{12}C$ breakup states of ^{24}Mg was carried out by Curtis *et al.* [15] which indicated a close overlap between the energies, spins, and widths of the breakup states with those of the scattering resonances. A greater understanding of the breakup reactions was provided by the Harvey model [16] which led to predictions [9] that four-particle–four-hole (4p-4h) transfer reactions were required to observe breakup of ^{32}S into $^{16}O+^{16}O$. The Harvey rules were later shown to emerge naturally from a model using a two-center deformed harmonic oscillator [17]. Using the $^{12}C(^{24}Mg,^{16}O^{16}O)\alpha$ reaction, Curtis *et al.* [18] provided evidence for a highly deformed dinuclear configuration in ^{32}S with a rotational parameter which followed the trend of the $^{16}O+^{16}O$ scattering resonances.

The experimental situation for cluster asymmetric nuclei such as ^{28}Si is more difficult, because there is an increased density of states for the breakup into nonidentical clusters which form natural parity bands with both even and odd spin sequences. This demands a higher experimental resolution for the states to be resolved. Bennett *et al.* [9] first observed breakup yield to unresolved states in ^{28}Si via the $^{12}C(^{24}Mg,^{12}C^{16}O)^8Be$ reaction, and later work by Freer [19], using the same reaction, obtained the spin of one state at an excitation of 30.0 MeV in ^{28}Si. Murgatroyd *et al.* [20] saw states of excitation energies of 30–40 MeV via the $^{12}C(^{20}Ne,^{12}C^{16}O)\alpha$ reaction, but were unable to resolve the states or to see any structure in the angular correlations.

Freer *et al.* [21] investigated the reactions of ^{16}O at 80.5 MeV and 99.0 MeV with both ^{12}C and ^{16}O targets and found evidence for a strong final state interaction to populate breakup states in ^{24}Mg and ^{28}Si. For the $^{12}C(^{16}O,^{12}C^{12}C)\alpha$ reaction, the angular correlations for ^{24}Mg determined the spins of four new states and, interestingly, these lay outside (and below) the locus of the scattering resonance on the plot of E_x vs $J(J+1)$. However, the yield for the $^{16}O(^{16}O,^{12}C^{16}O)\alpha$ reaction was a factor of 5 smaller, and most of the ^{12}C and ^{16}O coincidences were shown to arise from inelastic scattering from the carbon backing on the target, followed by breakup of the excited ^{16}O to $^{12}C+\alpha$. Hence, the excitation energy spectrum obtained for ^{28}Si at 80.5 MeV showed only unresolved peaks and no yield was obtained at 99 MeV. Further work by Shawcross [22] using the $^{12}C(^{24}Mg,^{12}C^{16}O)^8Be$, $^7Li(^{24}Mg,^{12}C^{16}O)^3H$, and $^8Be(^{24}Mg,^{12}C^{16}O)^5He$ reactions, at 170 MeV, has determined the spins of two states, which, like the state observed by Freer [19], appear to lie below the boundary of the locus of the scattering resonances [23–25].

The present work follows from the initial observations of Freer *et al.* [21] and uses the $^{16}O(^{16}O,^{12}C^{16}O)\alpha$ reaction at energies of 90 and 97 MeV to make new measurements of $^{12}C+^{16}O$ breakup of states in ^{28}Si using a lithium oxide target and a detector array which was optimized for this reaction. In Sec. II, the experimental setup is described, and in Sec. III some brief details of the analysis techniques are given, as well as a discussion of the results of the spin assignments made using angular correlation techniques, while Sec. IV compares the existing and present measurements in the context of some theoretical models using the two-center harmonic oscillator shell model [26,27] and the alpha-cluster model [28].

II. EXPERIMENT

This experiment was carried out at the Australian National University, Canberra. The 14UD tandem Van de Graaff accelerator was used to accelerate ^{16}O ions onto a Li_2O (100 μg cm^{-2}) target mounted on a ^{12}C backing (10 μg cm^{-2}), producing the reaction ^{16}O(^{16}O,^{28}Si)α with a Q value of -7.16 MeV. This leads to the breakup of the ^{28}Si compound nucleus, with the observed channel being ^{12}C+^{16}O ($Q=-16.76$ MeV). Beam energies of 90 MeV and 97 MeV were used.

The breakup fragments from the reaction were detected by two gas-Si hybrid detectors [29] placed asymmetrically on either side of the optical beam line in the scattering chamber. At $E_{beam}=90$ MeV detector 1 was at a polar laboratory angle of 21.4° and detector 2 was at 27.6°. At $E_{beam}=97$ MeV the angles were 30.2° and 23.6°, respectively.

The detectors were placed asymmetrically about the beam axis so that the breakup fragments could be observed efficiently at both beam energies. As ^{16}O is the heavier of the two breakup products it will be projected at more forward angles than the lighter ^{12}C, thus requiring one detector at a forward angle to pick up the ^{16}O and the other detecting the ^{12}C. It is still possible to record coincidences with the ions in the other detectors, although the efficiency is lower in this case.

The hybrid detectors used in this experiment consist of a longitudinal ionization chamber, with a Mylar window, and a 16-element position sensitive silicon strip detector (PSSSD). They are similar to detectors used in other experiments [15,30–32] carried out by the CHARISSA Collaboration.

III. ANALYSIS AND RESULTS

To analyze these data the resonant particle spectroscopy (RPS) technique was used, first proposed by Robson [33] and developed by Rae [34]. This method is used to provide a full kinematic reconstruction of breakup reactions.

The three-body Q value is defined as the difference between the kinetic energy of the reaction and the beam energy, and is given by

$$Q=(E_1+E_2+E_{recoil})-E_{beam}, \tag{1}$$

where E_1 and E_2 are the energies of the breakup fragments.

The final total energy spectrum, which is the energy of the three final state particles, reveals a peak, denoted Q_{ggg}, which corresponds to all three decay products emerging in their ground states. For $E_{beam}=90$ MeV the centroid of the Q_{ggg} peak is at (82.65±0.01) MeV which is in good agreement with the expected value of 82.57 MeV. For $E_{beam}=97$ MeV the centroid of the Q_{ggg} peak is at (89.87±0.01) MeV which is also in good agreement with the expected value of 89.58 MeV. The total energy spectrum for 90 MeV is shown in Fig. 1. A Monte Carlo simulation [35] of the reaction and detection processes indicates an energy resolution of 1.6 MeV [full width at half maximum (FWHM)] in reasonable agreement with the measured experimental value of 2.2 MeV.

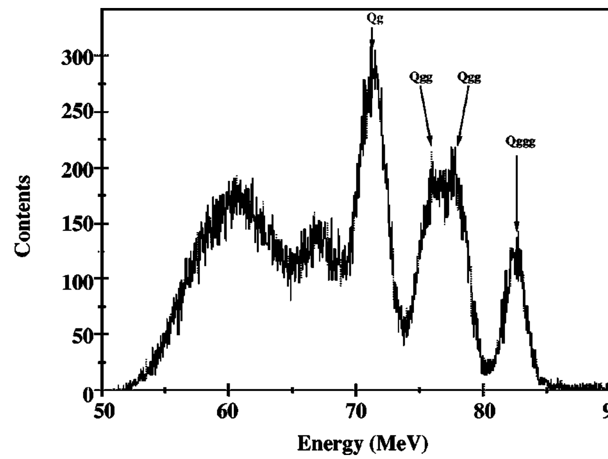

FIG. 1. The total energy spectrum for the ^{16}O(^{16}O,^{12}C^{16}O)α reaction at $E_{beam}=90$ MeV.

Selecting events within the Q_{ggg} peak allows the rejection of any exit channel particles which are in their excited states. The excitation energy (E_x) of the resonant nucleus can then be obtained from the relative energy of the breakup particles (E_{rel}) and the two-body Q value ($Q_{12}=16.7$ MeV for the ^{12}C+^{16}O breakup of ^{28}Si) for the breakup reaction, i.e.,

$$E_x=E_{rel}+Q_{12}. \tag{2}$$

However, particles detected in the experiment may not come from the ^{28}Si resonant nucleus, but from the breakup of other nuclei, leading to states created by the final state interactions between the breakup and recoil particles. Plotting the relative energy between the ^{12}C and α nuclei against the relative energy between the ^{16}O and the α nuclei will produce spectra, such as that shown in Fig. 2, with horizontal, vertical, and diagonal loci. The horizontal and vertical loci show final state interactions between the breakup fragments and the recoil nucleus, which correspond to states in ^{16}O and ^{20}Ne. The vertical loci in Fig. 2 show states of 7.36, 10.50, and 15.69 MeV in ^{20}Ne and the horizontal loci show states of 8.83 and 13.16 MeV in ^{16}O. These correspond to known states in ^{20}Ne [36] and ^{16}O [37] that decay by α emission. The diagonal loci are the final state interactions of the two detected fragments, i.e., states in ^{28}Si. A gate, with lower limits of 21.0 MeV in E_{rel}(^{16}O-α) and 16.5 MeV in E_{rel}(^{12}C-α) (upper right quadrant in Fig. 2), was used select only those states which are found in the ^{28}Si nucleus, reducing any background created by states in the ^{20}Ne and ^{16}O nuclei. The projection of the spectrum, within this window, onto the x and y axes is also shown in Fig. 2. Outside the window the peaks correspond to the states seen in ^{16}O and ^{20}Ne. However, inside the window the spectra are featureless, indicating that there is no background from resonant states in ^{16}O or ^{20}Ne, and thus this data should correspond to the decay of states in ^{28}Si. The excitation energy spectra for ^{28}Si at beam energies of 90 and 97 MeV are shown in Figs. 3 and 4, respectively. The dashed lines in Figs. 3 and 4

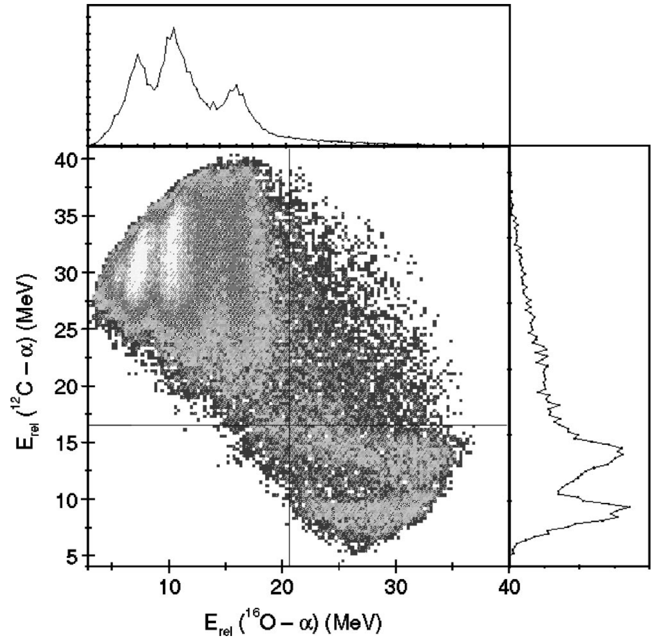

FIG. 2. Relative energy between each breakup product and the alpha for $^{16}O+{}^{12}C$ coincidences at $E_{beam}=90$ MeV. The software window used to select the states in ^{28}Si is the upper right quadrant. The spectrum on the *y* axis shows the projection of these data to the left of the line at 21 MeV and the spectrum on the *x* axis shows the projection above the line at 16.5 MeV.

indicate the detection efficiency determined by the Monte Carlo simulation code. Indicated are the peaks where angular correlations were taken and spin assignments found. These states were at 30.27 and 32.87 MeV at $E_{beam}=90$ MeV and at 32.81, 34.50, 36.60, and 37.87 MeV at $E_{beam}=97$ MeV. A region centered on 39.01 MeV was also analyzed at $E_{beam}=97$ MeV. Figures 3 and 4 show that only one state at $E_x=32.87$ MeV seems to be populated at both beam energies, despite similar efficiencies at the two energies. The state at $E_x=30.27$ MeV, which is strongly excited

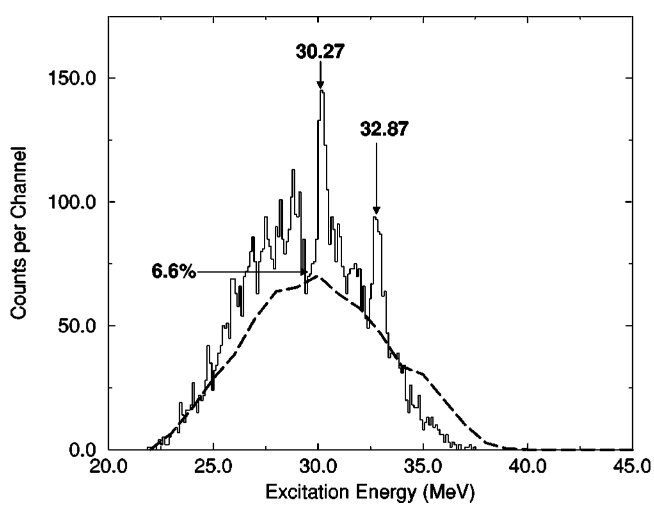

FIG. 3. Excitation energy spectra of ^{28}Si at $E_{beam}=90$ MeV. The dashed line represents the Monte Carlo simulation of the efficiency.

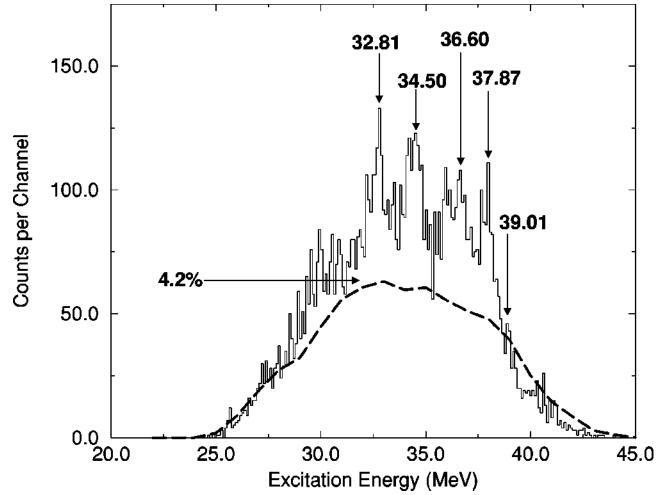

FIG. 4. Excitation energy spectra of ^{28}Si at $E_{beam}=97$ MeV. The dashed line represents the Monte Carlo simulation of the efficiency.

at 90 MeV, is only weakly excited at 97 MeV, and no angular correlation could be obtained to confirm the spin assignment made at 90 MeV. These rapid changes in the spectrum with a small change in energy are not consistent with a direct reaction mechanism which would produce smooth changes with energy, but suggest that these states are populated by resonances in the ^{32}S compound nucleus which α decay into states in ^{28}Si.

Angular correlations

Once a complete kinematic reconstruction of these data is achieved, then the angular momentum of the state may be extracted. To do this, an angular correlation technique is used. A two-dimensional plot of the angle (ψ) between the relative velocity vector (v_{rel}) and the beam axis is plotted against the emission angle (θ^*) of the ^{28}Si in the center-of-mass frame [11–14]. An example of this plot is shown in Fig. 5 for the state at 32.87 MeV.

In the reaction $^{16}O(^{16}O,{}^{12}C^{16}O)\alpha$, the two ^{16}O nuclei in the entrance channel have a spin of zero, so for $\theta^*=0$, the excited ^{28}Si nucleus will be in the $m=0$ magnetic substate. For this case the angular distributions of the ^{12}C and ^{16}O decay products from a particular state will be described by the square of a Legendre polynomial,

$$\frac{d^2\sigma}{d\theta^* d\psi} \propto |P_J(\cos\psi)|^2, \tag{3}$$

where the order of the polynomial (J) is the spin of the excited state of the ^{28}Si nucleus.

At scattering angles away from $\theta^*=0$ the ^{28}Si nucleus can be populated in other magnetic substates, with a variety of amplitudes contributing to the angular distributions. If, however, the contributions from nonzero magnetic substates vary slowly with scattering angle, the correlation becomes shifted [38,39], so that

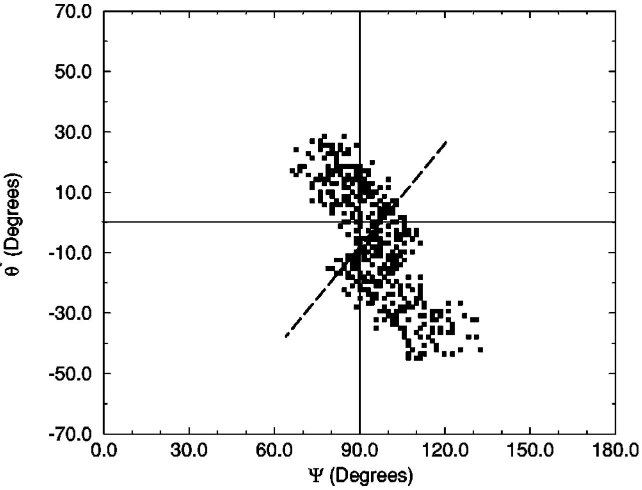

FIG. 5. Plot of θ^*-ψ for the state at $E_x = 32.87$ MeV at $E_{beam} = 90$ MeV. The solid lines represent $\theta^* = 0$ and $\psi = 90°$. The dashed line represents the angle of projection.

$$\frac{d^2\sigma}{d\theta^* d\psi} \propto |P_J[\cos(\psi + \Delta\psi)]|^2, \tag{4}$$

where $\Delta\psi = \Delta\theta^* l_f / J$ and l_f is the dominant angular momentum of the exit channel, usually taken as the grazing angular momentum.

If ψ is plotted against θ^*, a series of diagonal ridges is typically seen in these data. At the intercept point on the $\theta^* = 0$ axis the ridges will correspond to the maxima and minima of the function $|P_J(\cos\psi)|^2$.

To extract the spin of the nucleus, the order of the Legendre polynomial is selected so that the periodicity of the peaks in the polynomial matches those of the ridges when projected onto the $\theta^* = 0$ axis. The parity of the state will then be given by $\pi = (-1)^J$. Figure 6(a) shows the projection of the ridges seen in Fig. 5 onto the $\theta^* = 0$ axis.

The projected correlation for the state at 30.27 MeV is shown in Fig. 6. In this case the projection of these data onto the $\theta^* = 0$ axis, at two different angles, can be equally well described by $J = 9$ and $J = 11$. As these data are limited to a narrow band it is not possible to produce a unique spin assignment. The minimum at $\psi_0 = 90°$ indicates a state of negative parity which is also consistent with this assignment. These assignments are in good agreement with that of Freer [19] for the same state.

The state at 32.87 MeV can be seen in the excitation energy spectrum at both beam energies. However, angular correlations produced different spin assignments at each bombardment energy. At $E_{beam} = 90$ MeV a spin assignment of (11^-) was made and at $E_{beam} = 97$ MeV a spin of (12^+). The projection at each energy are shown in Figs. 7(a) and 7(b), respectively. There are two possible reasons for this discrepancy. Ambiguities will arise in the data due to the small widths of the bands formed in the angular correlation plots, such as that in Fig. 5. The angular correlation can thus be projected at different angles onto the $\theta^* = 0$ axis and thus different polynomials can fit these data; however, as these data span $\theta^* = 0$, the spin assignments always possess the same parity. The parity assignments for the peak at 32.87 MeV are different at each beam energy. One explanation for this is that a state of 11^- is populated at a beam energy of $E_{beam} = 90$ MeV, whereas at $E_{beam} = 97$ MeV a different, but unresolvable, state of 12^+ is populated. This would be consistent with the ideas of compound nucleus resonances in ^{32}S. The quality of the projection at $E_{beam} = 90$ MeV appears to indicate that a unique spin is not sufficient to describe these data.

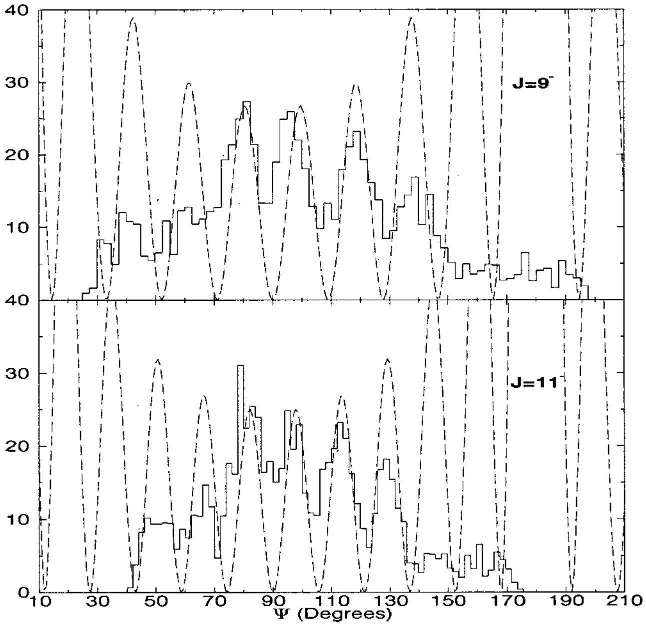

FIG. 6. Projection of the $\theta^* - \psi$ spectrum for the state at $E_x = 30.27$ MeV onto the $\theta^* = 0$ axis at $E_{beam} = 90$ MeV.

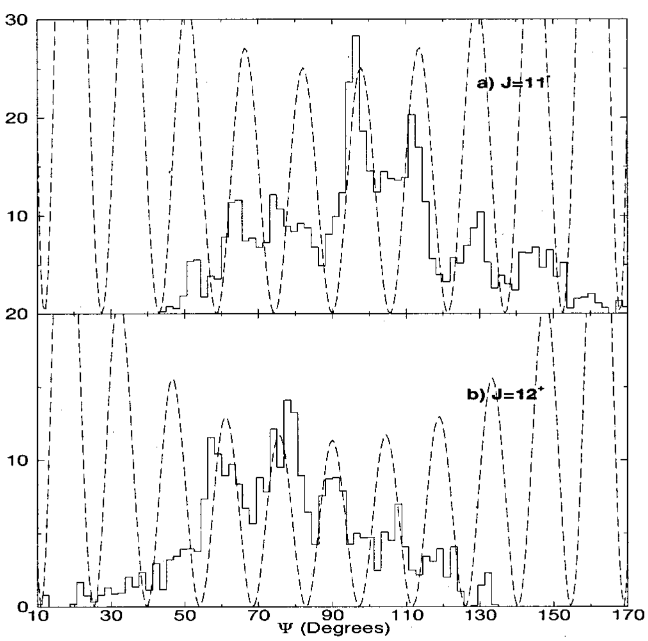

FIG. 7. Projection of the $\theta^* - \psi$ spectrum for the state at $E_x = 32.87$ MeV onto the $\theta^* = 0$ axis at (a) $E_{beam} = 90$ MeV and (b) $E_{beam} = 97$ MeV.

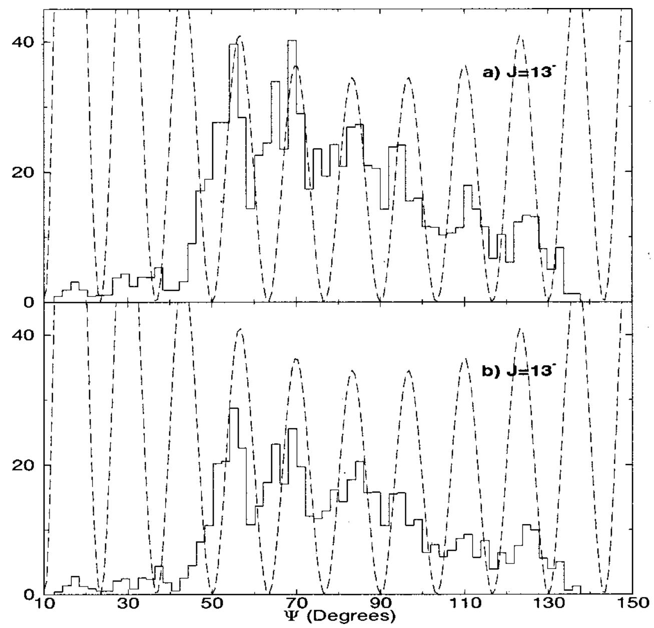

FIG. 8. Projection of the $\theta^* - \psi$ spectrum for the state at $E_x = 34.50$ MeV onto the $\theta^* = 0$ axis at $E_{beam} = 90$ MeV. (a) is the projection when gating over the whole of the peak and (b) is the projection of the right side of the peak.

Many of the measured states were found to have widths much larger than others. This could be evidence of unresolved (possibly mixed-spin) doublets. This results from the high density of states in ^{28}Si, where, unlike for the ^{24}Mg or ^{32}S cases previously studied, both odd and even spin states can be observed in the asymmetric breakup channel. As an example, Fig. 8(a) shows the state at 34.50 MeV with Legendre polynomials of order 13 superimposed. The minimum at $\psi_0 = 90°$ indicates that the state is of negative parity, which is consistent with a 13^- state. However, the peak seems to be split into two. A software window on the right side of the peak produced the angular correlation in Fig. 8(b). This correlation, with a minimum at $\psi_0 = 90°$, also indicates a negative parity and is consistent with a state with spin (13^-). This assignment is in good agreement with those of Shawcross [22] for the same state. In addition, a spin assignment of 16^+ (shown in Fig. 9) was also made for the state at 37.87 MeV.

We have investigated the background to the excitation spectrum by gating on all the regions between the visible peaks. In only *one* region, centered at $E_x = 39.01$ MeV of the spectrum at $E_{beam} = 97$ MeV, could we find a structured angular correlation (Fig. 10) where there was no dominant peak. A polynomial of order 17 has a good match with the periodicity of the ridges, and there is a minimum at $\psi_0 = 90°$ indicating negative parity, so that a spin of $J = (17^-)$ is tentatively assigned. One explanation for this structure in the correlation is that it reflects a set of unresolved states whose spins must be $J = 17$ (or close to this value). An alternative explanation is that the structure of the angular correlation results from interference arising from many overlapping states of different spins which produce a coherent pattern with the minimum at 90°. Except for this single region, we can be confident that the angular correlations are unaffected by the background spectrum under the peaks, and do not affect the spins assignments listed in Table I.

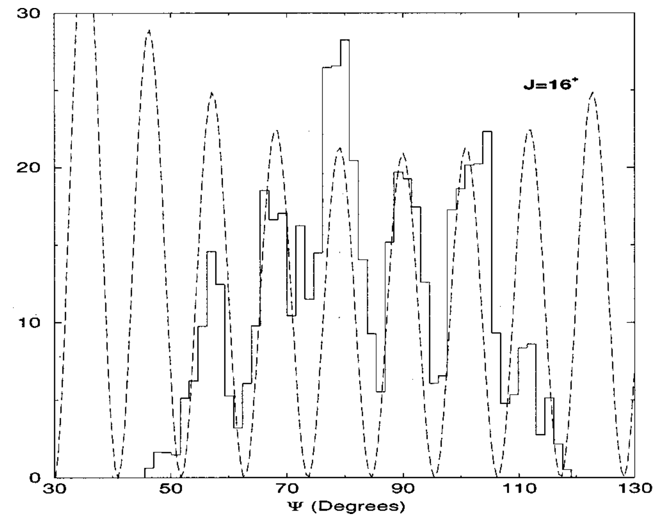

FIG. 9. Projection of the $\theta^* - \psi$ spectrum for the state at $E_x = 37.87$ MeV onto the $\theta^* = 0$ axis at $E_{beam} = 97$ MeV.

Table I summarizes the measured states for beam energies of 90 MeV and 97 MeV, respectively, with their corresponding spin assignments and widths. The Monte Carlo simulation of the energy resolution in the excitation energy spectrum yields a value of 206 keV (FWHM) at $E_x = 30$ MeV, consistent with the smallest values seen in this work. Also quoted is the grazing angular momentum of the entrance channel (l_{gi}). This is derived from the gradient of the ridges,

$$\frac{\Delta \theta^*}{\Delta \psi} = \frac{J}{l_f} = \frac{J}{l_{gi} - J}, \tag{5}$$

where l_f $(= l_{gi} - J)$ is the grazing angular momentum of the exit channel. Tentative assignments are shown in brackets.

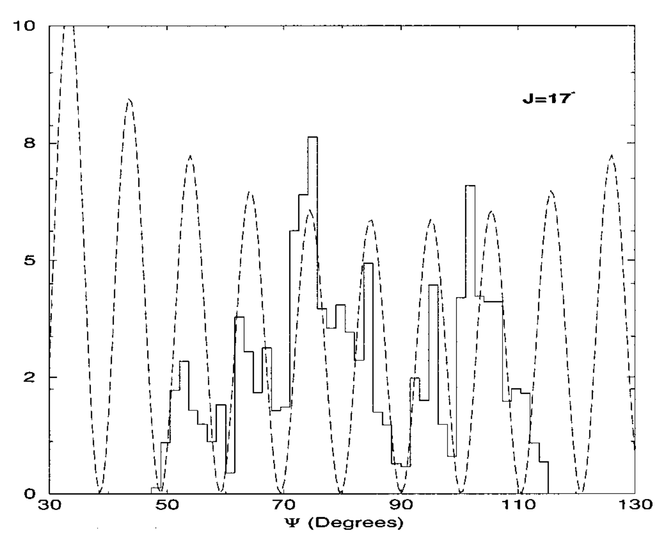

FIG. 10. Projection of the $\theta^* - \psi$ spectrum for the region at $E_x = 39.01$ MeV onto the $\theta^* = 0$ axis at $E_{beam} = 97$ MeV.

TABLE I. States observed via the $^{12}C+^{16}O$ breakup of ^{28}Si at $E_{beam}=90$ and 97 MeV, with corresponding spins, grazing angular momenta, and widths. Values in brackets are tentative spin assignments. The asterisk represents a possible mixed-state doublet.

Excitation energy (MeV)	J ($\hbar$)	E_{beam} (MeV)	Previous work	L_{gi} ($\hbar$)	Width (keV)
30.27 ± 0.02	$9^-,11^-$	90	$8^+,9^-$ [3]	21.39 ± 1.82	798 ± 66
			$(11^-\pm1)$ [19]		
32.81 ± 0.04	(12^+)	97		22.58 ± 1.69	854 ± 163
32.87 ± 0.02	(11^-)	90		19.39 ± 1.31	942 ± 78
34.50 ± 0.03	(13^-) [a]	97	$12^+,14^+$ [22]	26.00 ± 1.82	1446 ± 170*
	(13^-) [b]		$8^+,10^+$ [2]	26.00 ± 1.88	
36.60 ± 0.06	(10^+)	97	12^+ [3]	22.89 ± 1.82	293 ± 123
37.87 ± 0.04	16^+	97	11^- [3]	23.63 ± 1.40	892 ± 433
39.01 ± 0.06	(17^-) [c]	97		25.66 ± 1.96	

[a]When gating over all of the peak.
[b]When gating over the right hand side of the peak.
[c]When gating over a region centered on 39.01 MeV.

IV. DISCUSSION

The measured spin assignments (Table I) show that there is good agreement with both the scattering resonances [2,3] and previous breakup data [19] for the state at $E_x=30.27$ MeV. For example, the spin assigned to the 34.50 MeV state (13^-) is in good agreement with that of Shawcross [22]. However, the assigned J values are greater than those of the scattering resonance data for excitations above $E_x=32.24$ MeV. Figure 11 shows an E_x vs $J(J+1)$ plot for the present data, the previous breakup data, and the scattering resonance data. At lower spins, many of the states seen in this present study are found within the envelope of the range of the scattering resonances. However, many of the assignments from both the present and the other breakup data fall slightly below the l_{gi} line for the scattering data and at the lowest energy limit of the scattering resonances. A similar result was obtained by Freer *et al.* [21] for some states in the $^{12}C+^{12}C$ breakup of ^{24}Mg.

Given that any states which are below the l_{gi} locus could not be seen in the scattering studies (because the flux in those angular momentum states goes into fusion), we are faced with two possibilities. Either the breakup and resonance states are the same, with the breakup results revealing the true spin-energy systematics, or the breakup is revealing an entirely different structure in ^{28}Si which corresponds to a much higher deformation. A best fit to an assumed rotational band, through all the points, gives a moment of inertia of (42 ± 5) keV and a bandhead energy of $E_x=(26.3\pm0.9)$ MeV, which is shown in Figs. 12 and 13.

A number of theoretical models predict the existence of highly deformed states in ^{28}Si. In the alpha cluster model (ACM) of Zhang, Merchant, and Rae [28], a rotational band corresponding to a 4:1 deformation of the ^{28}Si nucleus is observed, which is associated with a minimum in the potential energy surface in the Nilsson-Strutinsky calculations of Leander and Larsson [40]. The ACM calculation gives a moment of inertia for this band of (54 ± 1) keV and a bandhead energy of 30.6 MeV. The rotational parameter for the ACM

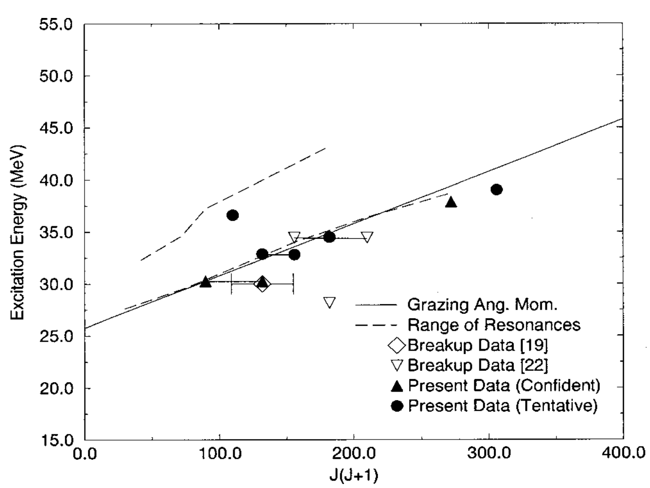

FIG. 11. A comparison between the present data and the breakup [19,22] and resonance data [2,3].

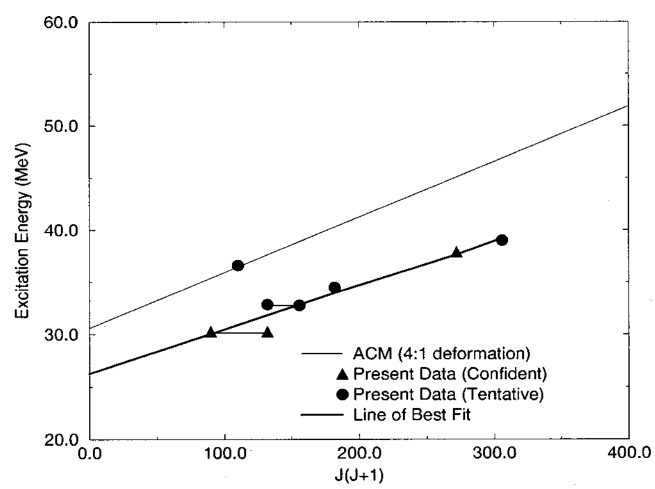

FIG. 12. A comparison between the present data and the ACM calculations for a 4:1 deformation in the ^{28}Si nucleus by Zhang *et al.* [28].

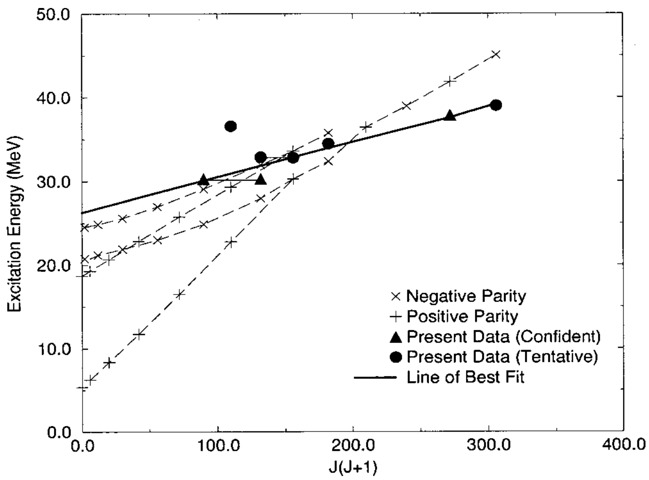

FIG. 13. A comparison between the present data and the two-center harmonic oscillator [26,27].

calculation is in excellent agreement with that of 55 keV calculated for two touching, spherical ^{12}C and ^{16}O nuclei (compared to 119 keV for a spherical ^{28}Si nucleus). Figure 12 shows a comparison of this band trajectory with the breakup states. The experimental data would indicate a band which is more deformed than a 4:1 deformed nucleus, since the gradient of the band is shallower.

An alternative model of states in ^{28}Si was proposed by Baye and Heenen [26,27] using the two-center harmonic oscillator (TCHO). This model predicts two bands each of both positive and negative parity, with different bandheads (see Fig. 13). While the negative parity bandheads are close to each other at $\sim$21 and $\sim$25 MeV, the positive bandheads are widely spaced at $\sim$5 and $\sim$18 MeV, and these bands merge with the corresponding negative parity bands at spin of $J=12^+$; thereafter there appears to be a consistent slope of 90 keV, with alternating positive and negative parity states lying on the same locus. Some of the lower spin assignments in this present work overlap the states produced by Baye and Heenen, but like the alpha cluster model, the predicted slope appears to be steeper than would be indicated by the higher spin states between 35 and 40 MeV found in the present work.

One possible explanation for our observation of a highly rotational band could be the presence of vibrational modes built upon one (or more) rotational bands. In this scenario, vibrational states (of low spin) at the lowest energies combined with high spin states of the rotational band at high energy could mimic the appearance of a band with a shallow gradient. However, the ACM does not consider the possibility of vibrational modes, and so we cannot eliminate this explanation. The TCHO model does consider vibrations, but its predictions do not agree with our data.

V. CONCLUSIONS

The breakup of ^{28}Si using the ^{16}O(^{16}O,^{12}C^{16}O)α reaction has been studied at energies of 90 and 97 MeV. At both energies excited states of ^{28}Si were identified and subjected to angular correlation analysis. A number of spin assignments were obtained from the angular correlations, with confident assignments of $J^\pi=16^+$ at 37.87 MeV and either 9^- or 11^- at 30.27 MeV. There is evidence of overlapping states for some of the observed peaks, which results in larger peak widths and leads to tentative spin assignments for states at 32.87 MeV $[J=(11^-,12^+)]$ and 34.5 MeV $[J=(13^-)]$. Only the state near 36.6 MeV $[J=(10^+)]$ showed a measured width of 293 keV, close to that predicted by the Monte Carlo simulations. The higher spin states were shown to lie below the grazing angular momentum in the entrance channel, and therefore cannot be seen in scattering resonances.

By gating in the background between the peaks, we were able to confirm that the background did not produce angular correlations underlying the peaks, except for a region centered on $E_x=39.01$ MeV in the spectrum obtained at $E_{beam}=97$ MeV, where the correlation was consistent with a spin of $J=(17^-)$. It is uncertain whether this arises from overlapping states with $J=17$ or constructive interference arising from the overlap of many states with different spins.

A comparison with both the alpha cluster model of Zhang *et al.* [28] and the two-center harmonic oscillator shell model of Baye and Heenen [26,27] shows that these models predict very different bandheads, but more importantly, the rotational slopes are predicted to be much steeper than the trend indicated by the present data. A best fit line through the centroid of the low spin states yields a rotational parameter of (42 ± 5) keV and a bandhead of (26.3 ± 0.9) MeV, and may indicate a highly deformed band populated by the breakup of ^{28}Si into ^{12}C$+^{16}$O.

ACKNOWLEDGMENTS

The authors would like to acknowledge the support and assistance of the staff at the Australian National University. This work was carried out under a joint EPSRC-ANU agreement. N.I.A., R.L.C., G.K.D., A.M., and M.S. would like to acknowledge financial support from EPSRC.

[1] K. A. Erb and D. Bromley, in *Treatise on Heavy Ion Science*, edited by D. Bromley (Plenum, New York, 1985), Vol. 3.
[2] N. Cindro, Ann. Phys. Fr. **13**, 289 (1988).
[3] N. Cindro, Riv. Nuovo Cimento **4**, No. 6 (1981).
[4] A. M. Sandorfi, J. R. Calarco, R. E. Rand, and H. A. Schwettman, Phys. Rev. Lett. **45**, 1615 (1980).
[5] C. A. Davies, G. A. Moss, G. Roy, J. Uegaki, R. Abegg, L. G. Greeniaus, D. A. Hutcheon, and C. A. Miller, Phys. Rev. C **35**, 336 (1987).
[6] S. Lawitski, D. Pade, B. Gonsior, C. D. Uhlhorn, S. Brandenburg, M. N. Harakeh, and H. W. Wilschut, Phys. Lett. B **174**, 246 (1986).
[7] J. Wilczynski, K. Siwek-Wilczynska, Y. Chan, E. Chaves, S. B. Gazes, and R. G. Stokstad, Phys. Lett. B **181**, 229 (1986).

[8] B. R. Fulton, S. J. Bennett, C. A. Ogilvie, J. S. Lilley, D. W. Banes, W. D. M. Rae, S. C. Allcock, R. R. Betts, and A. E. Smith, Phys. Lett. B **181**, 233 (1986).
[9] S. J. Bennett, M. Freer, B. R. Fulton, J. T. Murgatroyd, P. J. Woods, S. C. Allcock, W. D. M. Rae, A. E. Smith, J. S. Lilley, and R. R. Betts, Nucl. Phys. **A534**, 445 (1991).
[10] B. R. Fulton and W. D. M. Rae, J. Phys. G **16**, 333 (1990).
[11] B. R. Fulton, S. J. Bennett, M. Freer, J. T. Murgatroyd, G. J. Gyapong, N. S. Jarvis, C. D. Jones, D. L. Watson, J. D. Brown, W. D. M. Rae, A. E. Smith, and J. S. Lilley, Phys. Lett. B **267**, 325 (1991).
[12] M. Freer, Nucl. Instrum. Methods Phys. Res. A **383**, 463 (1996).
[13] M. J. Leddy, S. J. Bennett, N. M. Clarke, M. Freer, B. R. Fulton, J. T. Murgatroyd, G. J. Gyapong, C. D. Jones, D. L. Watson, W. D. M. Rae, A. E. Smith, and W. N. Catford, Nucl. Phys. **A589**, 363 (1995).
[14] E. Costanzo, M. Lattuada, M. Romano, D. Vinciguerra, N. Cindro, M. Zadro, M. Freer, B. R. Fulton, and W. D. M. Rae, Phys. Rev. C **44**, 111 (1991).
[15] N. Curtis, N. M. Clarke, B. R. Fulton, S. J. Hall, M. J. Leddy, A. St. J. Murphy, J. S. Pople, R. P. Ward, W. N. Catford, G. J. Gyapong, S. M. Singer, S. P. G. Chappell, S. P. Fox, C. D. Jones, D. L. Watson, W. D. M. Rae, and P. M. Simmons, Phys. Rev. C **51**, 1554 (1995).
[16] M. Harvey, in Proceedings of the 2nd International Conference on Clustering Phenomena in Nuclei, College Park, Maryland, 1975, edited by D. A. Goldberg, USDERA Report No. ORO-4856-26, 1975 (unpublished), p. 549.
[17] M. Freer, R. R. Betts, and A. H. Wousmaa, Nucl. Phys. **A587**, 36 (1995).
[18] N. Curtis, A. St. J. Murphy, N. M. Clarke, M. Freer, B. R. Fulton, S. J. Hall, M. J. Leddy, J. S. Pople, G. Tungate, R. P. Ward, W. N. Catford, G. J. Gyapong, S. M. Singer, S. P. G. Chappell, S. P. Fox, C. D. Jones, D. L. Watson, W. D. M. Rae, P. M. Simmons, and P. H. Regan, Phys. Rev. C **53**, 1804 (1996).
[19] M. Freer, invited talk at 6th International Conference on Clusters in Nuclear Structure and Dynamics, Strasbourg, France, 1994.
[20] J. T. Murgatroyd, S. J. Bennett, B. R. Fulton, J. S. Pople, N. S. Jarvis, D. L. Watson, and W. D. M. Rae, Phys. Rev. C **51**, 2230 (1995).
[21] M. Freer, N. M. Clarke, R. A. Le Marechal, G. Tungate, and R. Ward, Phys. Rev. C **51**, 3174 (1995).
[22] M. Shawcross, Ph.D. thesis, University of Surrey, 1999.
[23] F. P. Brady, D. A. Viggars, T. W. Conlon, and D. J. Parker, Phys. Rev. Lett. **39**, 870 (1977).
[24] F. Soga, J. Schimizu, H. Kamitsubo, N. Takahashi, K. Takimoto, R. Wada, F. Fujisawa, and T. Wada, Phys. Rev. C **18**, 870 (1978).
[25] D. Branford, B. N. Nagorcka, and J. O. Newton, J. Phys. A **7**, 1565 (1977).
[26] D. Baye, Nucl. Phys. **A272**, 445 (1976).
[27] D. Baye and P. H. Heenen, Nucl. Phys. **A283**, 176 (1977).
[28] J. Zhang, A. C. Merchant, and W. D. M. Rae, Nucl. Phys. **A575**, 61 (1994).
[29] N. Curtis, A. St. J. Murphy, M. J. Leddy, J. S. Pople, N. M. Clarke, M. Freer, B. R. Fulton, S. J. Hall, G. Tungate, R. P. Ward, S. M. Singer, W. N. Catford, G. J. Gyapong, R. A. Cunningham, J. S. Lilley, S. P. G. Chappell, S. P. Fox, C. D. Jones, D. L. Watson, P. M. Simmons, R. A. Hunt, A. C. Merchant, A. E. Smith, W. D. M. Rae, and J. Zhang, Nucl. Instrum. Methods Phys. Res. A **351**, 359 (1994).
[30] M. Freer, Ph.D. thesis, University of Birmingham, 1991.
[31] P. J. Leask, Ph.D. thesis, University of Birmingham, 2000.
[32] S. M. Singer, Ph.D. thesis, University of Surrey, 1996.
[33] D. Robson, Nucl. Phys. **A204**, 523 (1973).
[34] W. D. M. Rae, Phys. Rev. C **30**, 158 (1984).
[35] N. Curtis, computer code RESOLUTION 8, Ph.D. thesis, University of Birmingham, 1995.
[36] F. Ajzenberg-Selove, *Energy Levels of Light Nuclei A=18–20* (North-Holland, Amsterdam, 1987), Vol. A475, No. 1.
[37] F. Ajzenberg-Selove, *Energy Levels of Light Nuclei A=16–17* (North-Holland, Amsterdam, 1982), Vol. A375, No. 1.
[38] E. F. Da Silviera, Proceedings of the 14th Winter Meeting on Nuclear Physics, Bormio, 1976 (unpublished).
[39] S. Marsh and W. D. M. Rae, Phys. Lett. **153B**, 21 (1985).
[40] G. Leander and S. E. Larsson, Nucl. Phys. **A239**, 93 (1975).